Eksploatacja i Niezawodnosc – Maintenance and Reliability
Volume 23 (2021), Issue 3
journal homepage: http://www.ein.org.pl
Article citation info:
Castilla-Gutiérrez J, Fortes Garrido JC, Davila Martín JM, Grande Gil JA. Evaluation procedure for blowing machine monitoring and predicting bearing SKFNU6322 failure by power spectral density. Eksploatacja i Niezawodnosc – Maintenance and Reliability 2021; 23 (3): 522–529, http://doi.org/10.17531/ein.2021.3.13.

Evaluation procedure for blowing machine monitoring and predicting bearing SKFNU6322 failure by power spectral density

Indexed by: Web of Science Group

Javier Castilla-Gutiérrez[b], Juan Carlos Fortes Garrido[a,b], Jose Miguel Davila Martín[a,b,*], Jose Antonio Grande Gil[a,b]

[a] Department of Water, Mining and Environment. Scientific and Technological Centre of Huelva, University of Huelva, 21007 Huelva, Spain
[b] Sustainable Mining Engineering Research Group. Department of Mining, Mechanic, Energetic and Construction Engineering. Higher Technical School of Engineering, University of Huelva, 21007 Huelva, Spain

Highlights

- Comparative study of characteristic frequencies in terms of Power Spectral Density.
- Monitoring of blower unit and the SKFNU322 bearing.
- A new predictive maintenance protocol has been develop.
- The method used allows reducing from 6 control points to one.

Abstract

This work shows the results of the comparative study of characteristic frequencies in terms of Power Spectral Density (PSD) or RMS generated by a blower unit and the SKFNU322 bearing. Data is collected following ISO 10816, using Emonitor software and with speed values in RMS to avoid high and low frequency signal masking. Bearing failure is the main cause of operational shutdown in industrial sites. The difficulty of prediction is the type of breakage and the high number of variables involved. Monitoring and analysing all the variables of the SKFNU322 bearing and those of machine operation for 15 years allowed to develop a new predictive maintenance protocol. This method makes it possible to reduce from 6 control points to one, and to determine which of the 42 variables is the most incidental in the correct operation, so equipment performance and efficiency is improved, contributing to increased economic profitability. The tests were carried out on a 500 kW unit of power and It was shown that the rotation of the equipment itself caused the most generating variable of vibrational energy.

Keywords

vibration; bearing failure; diagnostics; failure analysis; power spectral density.

1. Introduction

Bearing failure is one of the most important causes of industrial equipment shutdown, in fact it is estimated that 40% of shutdowns are generated by bearings [28, 42]. Bearing failure is caused by many factors, such as lubrication, loads, handling failures, lack of preventive maintenance, among others [10, 34, 39].

ISO 10816-3 establishes that there are four stages of breakage, which are caused by unbalance, or misalignment [24, 32, 8]. Determining the stage is one of the main objectives of predictive maintenance and of industries in general, which are looking for this new technology to reduce the problem of production stoppages and the cost associated to them [4, 36]. Finding the breakage moment is the main objective, but the breakage type in the form of a ski curve makes this very difficult, because the transition from the third to the fourth stage takes place in a brief period of time involving corrective actions [18, 27]. Another problem is the number of fault types [22].

New non-invasive techniques, such as acoustic study, are trying to improve predictive maintenance [21, 23], but involve environmental problems. The approach by spectral analysis of the vibrations is the most widespread technique, but it requires several control points and daily monitoring, resulting in a large cost in terms of time and personnel [20]. Other approaches experiment with vector support machines (SVM) and Wavelet signal processing [1, 5].

Current studies determine the type of defect in the laboratory. The problem arises when it is analysed under real working conditions [9, 12, 13]. In order to validate the method, it is necessary to have very large control samples, which allow to discriminate external factors. Therefore, this research evaluates equipment monitoring over a 15-year period.

Although there is some background of similar studies to the one done here, none of them are applied to equipment of such a large size and power as used in this research, and in no case, those studies have been extended over such a long period of time. Thus, some research found have been applied in a small blowing machines for bottles [17, 37] evaluating the software used, and those carried out by [15, 38] in wind turbines, in which the data acquisition has been developed for less than three years.

(*) Corresponding author.
E-mail addresses: J. Castilla-Gutiérrez - javier.castilla@dimme.uhu.es, J. C. Fortes Garrido - jcfortes@uhu.es, J. M. Davila Martín - jmdavila@dimme.uhu.es, J. A. Grande Gil - grangil@dimme.uhu.es

2. Materials and methods

2.1. Equipment under study

It has been studied an air blower and the bearing SKFNU322, which supports the mechanical drive shaft between the blades and the motor. The driving system is a motor, model Framesize 400, 3190 kg and 1.9 x 0.9 metres. All this can be seen in Figure 1.

The blade system measures 2.075 meters in diameter and the connection between the two is made by a 0.095-metre diameter and 3.9-metres-long shaft. This equipment belongs to Atlantic Copper company.

Many studies on bearing vibration analysis have been carried out, since operational safety and efficiency, together with environmental protection, is one of the challenges of the world's industry (McFadden and Smith 1984). Therefore, efforts are being made to meet this need through spectral vibration analysis [7, 14].

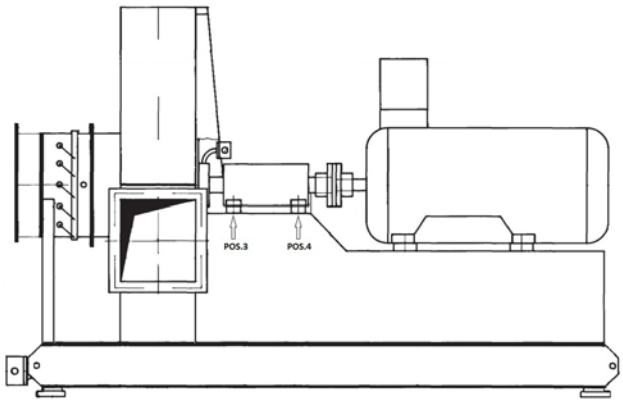

Fig. 1. Equipment in studio

The dynamic state of movement and the actual operating conditions are the major milestones in laboratory studies. They analyse bearing failures [25, 40], but their approximations are not valid for real operating conditions.

Mechanical vibration is a set of impulses caused by hitting moving elements on coinciding areas. These energy effects under constant operating conditions generate stable frequency disturbances, which can be determined and discriminated according to the element that generates them [11]. Each bearing is made up of a cage, balls and tracks, and the impact between them generates different periodic waves, which have their own spectral range [6, 38].

The fault frequency of the components of bearing SKFNU322 is defined according to the contact points [19]. The service life of different bearing components is determined by the amplitude of a specific disturbance. The existing types and the mathematical expressions that define them are the following:

- The movement of rotation of the balls or rollers around their axis is what defines the frequency of rotation of each of them (Eq. 1):

$$BSF = 0.5\ N \times (D/d) \times \left[1 - (d/D)^2\right] \tag{1}$$

- To determine the frequency of the ball defect, the so-called rotational frequency will be used, that is, twice the frequency of rotation of the balls or rollers (BSF), produced by the ball hit with both races (external and internal) at every turn (Eq. 2):

$$2BSF = N \times (D/d) \times \left[1 - (d/D)^2\right] \tag{2}$$

- The defect frequency of the ball support or rotation body (FTF) can be determined with the equation (3):

$$FTF = 0.5\ N \times \left[1 - (d/D)\right] \tag{3}$$

- The defect frequency produced in the ball passage or internal race (BPIR) and the defect frequency produced in the outer race or ball passage (BPOR) care calculated with the expressions (4) and (5) respectively:

$$BPIR = 0.5\ N\ n \times \left[1 - (d/D)\right] \tag{4}$$

$$BPOR = 0.5\ N\ n \times \left[1 - (d/D)\right] \tag{5}$$

Where:

- N is the angular speed of the axis in revolutions per second (rpm),
- D is the average bearing diameter (inches),
- d is the diameter of the rolling circumference of the balls or rollers (inches) and
- n is the number of rollers or balls forming the bearing.

- The blade frequency (Fpa) is the frequency generated by the blade passage and can be determined by the equipment rotational speed (RPM) and the blades number (Na) by using de equation (6):

$$Fpa = Na \times [RPM/60] \tag{6}$$

SKFNU322 bearing consists of 5 characteristic elements or frequencies, which are BSF, FTF, BPIR and BPOR, respectively. Another very important variable is 2BSF, which is generated by the second harmonic of the balls [30].

The equipment uses the SKFNU322 bearing as a support for the power transmission shaft, between the motor and the blades. Table 1 shows the fundamental characteristics of the bearing.

Table 1. Characteristics of bearing SKFNU322

Basic dynamic load (C)	C 530 kN	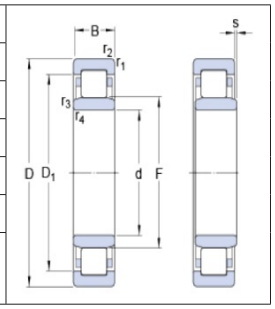
Basic static load (C0)	C0 540 kN	
Fatigue limit load (Pu)	Pu 61 kN	
Reference speed	3000 r/min	
Speed limit	3400 r/min	
Calculation factor (kr)	0.15	
Geometric characteristics	d = 110 mm; D = 240 mm; B = 50 mm; d1 ≈ 200 mm; F = 143 mm; r1,2,3,4 min. 3 mm	

They have been followed the guidelines of the ISO 10816.3 standard [43], to obtain the frequency spectra of the SKFNU322 bearing variables and the equipment fundamentals such as the blades and SPEED. The frequencies can be seen in the table below (Table 2).

2.2. Vibration analysis

Predictive maintenance is largely based on advances in the processing of vibration signals, through the frequency spectra and the power density spectra generated by these signals. The mathematician Jean Baptiste Fourier has formulated the relationship of the generated waves as a function of frequency instead of time (Eq. 7) [16]:

Table 2. Characteristic frequencies of the bearing under study (Hz)

Characteristic frequencies	Frequencies (Hz)
FTF	601.96
BSF	3735.4
2BSF	7470.9
BPOR	8425.9
BPIR	12434.0
SPEED	1490.0
BLADES	13410.0

$$X(f) = \int_{-\infty}^{\infty} x(t) * e^{-j2\pi ft} dt \tag{7}$$

The improvement of the Fast Fourier Transform (FFT) allows to avoid signal masking or aliasing, in signals of small amplitude. The PSD or Power Spectral Density (e.g. applied in [26] and [33]), is the energy that has each characteristic frequency, this follows the mathematical expression below (Eq. 8):

$$PSD(x(i)) = (1/T)\sum(x(i))^2 \Delta T \tag{8}$$

The sum x(i) for ΔT is the mean power of the interval. One way of estimating this energy is to limit the integration interval. It has been used a window based on the sample. This window is determined by the period o gram and allows to analyse hidden frequencies, avoiding signal masking [35].

The Hilbert HT transform (Hilbert Transform) studies the signal envelope. It achieves an improved PSD, making it easier to sample signals at low frequencies [31].

The method follows the procedure of transforming two functions s(t) and 1/(лt) into a third one, see the following mathematical expression (Eq. 9):

$$\bar{x}(t) = \frac{1}{\delta} \int_{-\infty}^{\infty} x(u) \frac{1}{t-u} du \tag{9}$$

The amplification of the signal envelope, for low frequency vibrations, provides improvements and disadvantages such as sensitivity to noise [29]. This was solved by the Wavelet Transform (WT), which provides information on signal processing such as time and frequency [41].

2.3. Data acquisition and processing

The study covers a period of 15 years, using Entel IRD and Odyssey Emonitor software for data acquisition and analysis. The measurement equipment has 16 channels with a nominal voltage of 24 V and 3.6 mA current.

The investigation was carried out on a 500 kW of power blowing machine with 3 m blades in a real operating conditions (constant regime) for 15 years and it was made by accredited technicians according to standard 18436-2, this fact makes this study unique in its category.

There are 4 filters used through a multiplexer, which generates acceleration, velocity and displacement signals. The accelerometer used has a sensitivity level of 100 mV/g., with a frequency range of 10000 Hz. The analogue-digital converter captures up to 51.2 kHz, with a resolution of 16 bit.

Monitoring is done through a magnetized anchor with quick release, which allows to reach faults with a frequency and sensitivity range between 0-300 Hz. A window of 3200 lines is used, with a range of 60000 to 300000 lines, depending on whether it is for speed or acceleration. The resolution of the Hanning window will be between 18 and 194 CPM, depending on the type of variable analysed (speed or acceleration).

According to the ISO 10816 standard, there are four levels of functional risk. For an equipment with flexible shaft, with power over 300 kW and speed of 1500 rpm, there would be an operating level that ranges from 0.18 to 11 RMS (mm/s), and its critical value is 7.1 RMS (mm/s), where corrective maintenance must be applied.

The ISO 10816 Standard, used for the diagnosis of vibration functionality in industrial equipment, determines that the evaluation should be done by the spectral level based on speed, as opposed to the use of acceleration or displacement, which only act properly at high or low frequency, respectively.

Integration considers the vibration signals produced at low frequency, acting to a lesser extent on those of high frequency. This is due to the proportional invertibility of the speed *V(f)* as a function of frequency *f*, see the following expression (Eq. 10):

$$V(f) = \frac{c_1 \ A(f)}{f} \tag{10}$$

The *D(f)* shift is also affected by the frequency in an exponential way (Eq. 11):

$$D(f) = \frac{c_2 \ A(f)}{f^2} \tag{11}$$

where *A(f)* is the acceleration of frequency *f* and C_1 and C_2 are constants.

The equipment has 2 sampling points for data acquisition, these are called POS3 and POS4. In each of them, data are collected in the three space coordinates, identified as POS3H, POS3V and POS3A for the third position and the horizontal, vertical and axial axes, respectively. The monitoring of point 4 follows the same rule.

According to the indications of the standard 10816-3, there are three maximum levels that dictate the correct operation of the equipment. For this analysis, a total of 617 shots are obtained for each of the two positions and the three coordinated axes, resulting in a total of 3702 data. This data discriminates the variable, the position and the axis that are most decisive and influential in the operation of the equipment.

As a summary, Figure 2 includes a diagram with the procedure used.

3. Results and discussion

In the first instance, the characteristic frequencies of the SKF-NU322 bearing in positions 3, 4 and their respective Cartesian axis are analysed. Within each position, the most critical axis is evaluated and compared with the other measurement position.

After the analysis of each frequency separately, they are all compared in their most sensitive positions to determine three fundamental elements, which would be the most harmful variable for the machine, its position and its axis.

Once the most sensitive variable of the bearing has been identified, it is related to the characteristic frequencies of the SPEED and Blades bearing in their most decisive control positions.

The analysis of the FTF frequency, generated by the bearing cage, is obtained by calculating the sum of values of the entire spectrum, at each of the control points. It is also done with the mean and the maximum or peak value, all in RMS.

For accumulated values and peak at position 3, the vertical axis is the most sensitive. When evaluating position 4, it has been obtained a value identical to the previous one. If the PO3V and POS4V points

are compared, it can be seen how it is in this latter position where the effect of the FTF frequency is greater, both in maximum accumulated values and in peak values, see Table 3.

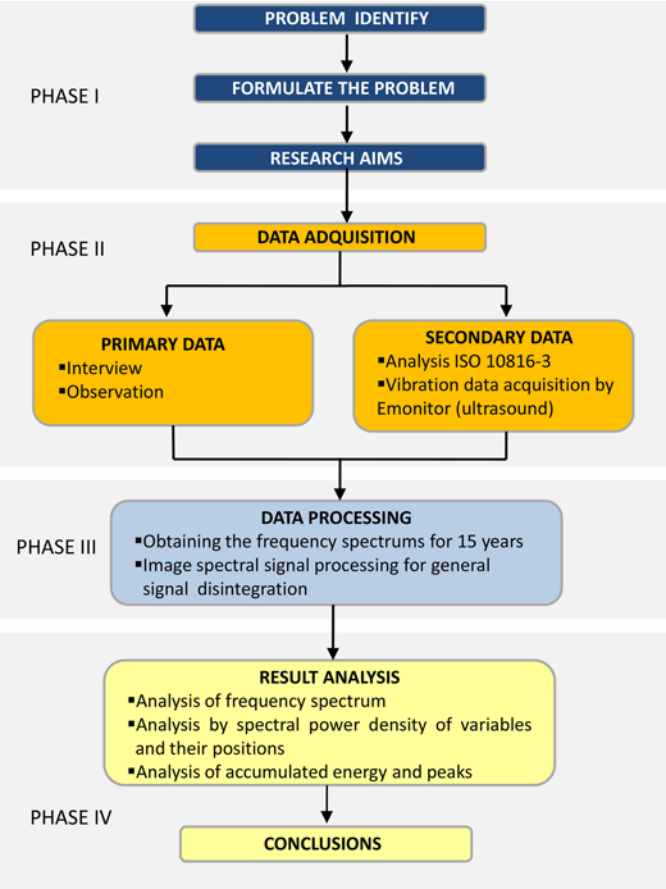

Fig. 2. Diagram with the procedure

Table 3. FTF result in terms of RMS (mm/s)

Variable	POS3H	POS3V	POS3A	POS4H	POS4V	POS4A
Total sum	52.480	55.880	51.590	94.970	9.480	59.040
Average	0.090	0.080	0.100	0.170	0.159	0.110
Peak value	0.520	1.340	0.560	7.610	7.747	1.180

In the analysis by values, the vertical axis of position 4 is the most important one to predict the failure of the frequency generated by the ball cage.

To fully validate the method, the FTF result on POS3 and POS4 is graphically compared to the vertical axis. The aim is to see if there is concordance and symmetry between the two, which allows us to state with complete certainty that the failure can be predicted, just analysing one of them.

Figure 3 shows that there is linearity between both and how it is in POS4V where the highest values are reached. This determines that it would be possible to predict the failure of this frequency, analysing only one of the six sampling positions.

It is important to highlight the ski curve effect, going from perfect operation values to breakage values higher than 7.1 RMS on days.

Once the FTF has been evaluated, BSF is analysed, starting from the third position and its axes, where the highest accumulated value and peak is obtained, which would be on the axial axis, with 47.7 RMS and 0.692 RMS, respectively. It has been obtained more incidence in the axial axis than in the vertical one, this indicates that position 3 is more sensitive to the vibration effect of this variable.

In the case of position 4, the vertical axis is the most important, followed by the axial and finally the horizontal axis. When comparing both positions, it can be seen how the axial and vertical axes are the most important, but in absolute terms POS4V that is the most decisive. Table 4 shows everything.

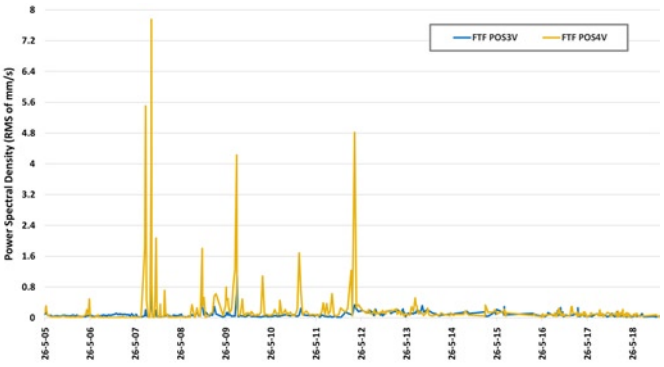

Fig. 3. FTF result in terms of RMS(mm/s) in positions 3 and 4 vertical

Table 4. BSF result in terms of RMS (mm/s)

Variable	POS3H	POS3V	POS3A	POS4H	POS4V	POS4A
Total sum	29.246	38.188	47.724	41.482	56.812	48.113
Average	0.048	0.062	0.078	0.068	0.093	0.089
Peak value	0.573	0.672	0.692	0.933	0.727	0.627

The variable generated by the bearing balls follows a common pattern in positions 3 axial and 4 vertical, even though they have different axes. The vertical axis of position 4 is the highest. In terms of peak values, they are very equal in both positions.

The graphical analysis indicates that both positions are important and should be monitored, because it is not always the vertical axis that produces the highest peak value.

When this result is compared with that obtained by the BSF variable, it is determined that the peak value in the latter reaches 7.1 RMS. However, in the variable generated by the balls, the peak value of the vertical axis is 0.727 RMS, which is within the optimum working conditions. This indicates that this variable is not the cause of bearing failure or breakage. All this can be seen in Figure 4.

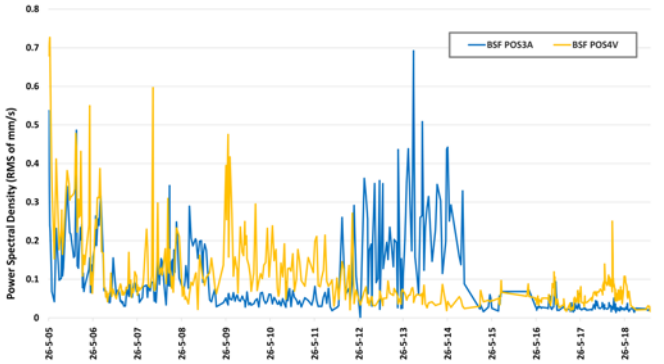

Fig. 4. BSF result in terms of RMS (mm/s) at positions 3 axial and 4 vertical

The BPOR analysis, in position 3, is the first variable where the most important effect is found in POS3H, its accumulated value is slightly higher than POS3V and both are very distant in relation to the axial axis.

Peak values are the same as cumulative values. It should be noted that these do not reach the risk values, as determined by the applied standard.

In position 4, the most sensitive axes are the horizontal and the axial, both in peak values and in accumulated values. It should be noted that in position 3 the values do not reach the risk values for the machine's operation.

The analysis of the BPOR frequency in accumulated values determines that POS3V is the most sensitive in position 3, and in the case of position 4, it is obtained in POS4A. The comparison of both determines that position 4 is the most decisive. All the above is shown in Table 5.

Table 5. BPOR result in terms of RMS (mm/s)

Variable	POS3H	POS3V	POS3A	POS4H	POS4V	POS4A
Total sum	19.343	16.388	10.507	20.647	16.503	28.448
Average	0.032	0.027	0.017	0.034	0.027	0.053
Peak value	0.346	0.213	0.099	0.307	0.272	0.411

The variable generated by the balls in the outer track of the bearing follows a common pattern in POS3H and POS4A positions, even though they have different axes. When comparing the graph, It has been obtained linearity between both positions and axes, this determines that the most severe action is the one perceived by POS4A, as shown in Figure 5.

The study of the BPIR variable on axis 3 determines that the most sensitive axis in cumulative values and peaks is the axial, followed by the vertical position. In the case of position 4, It has been obtained that the most important axis is the horizontal one, followed at great distance by the vertical one.

It should be noted that the effect between the axial and vertical axes of position 3 is closer, in cumulative terms, than those obtained between the horizontal and vertical axes of position 4.

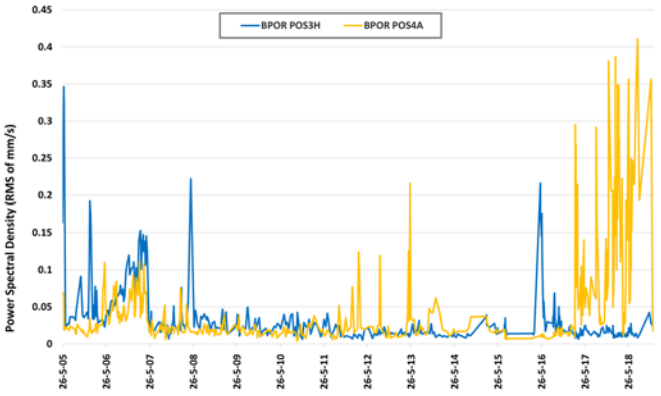

Fig. 5. BPOR result in terms of RMS(mm/s) at positions 3 horizontal and 4 axial

The analysis of the peak values determines that the axes 3 axial and 4 horizontal are the most important, but these do not reach values higher than 0.6 RMS, well below the critical 7.1, established by the existing legislation.

When comparing both positions, the result is that the axial position 3 is the one that perceives most the vibration effect of this variable, followed very closely by the horizontal position 4, with a little more than 1 RMS of difference. The same result is obtained in terms of peak values. Table 6 shows everything.

The variable generated by the balls in the inner track of the bearing follows a common pattern in POS3A and POS4H positions, even though they have different axes. This result is important because the linearity between both control points and determines that monitoring is possible by observing either of them, as shown in Figure 6. The

Table 6. BPIR result in terms of RMS (mm/s)

Variable	POS3H	POS3V	POS3A	POS4H	POS4V	POS4A
Total sum	36.364	42.149	52.048	51.198	29.070	18.113
Average	0.059	0.069	0.085	0.084	0.052	0.034
Peak value	0.456	0.542	0.593	0.482	0.426	0.147

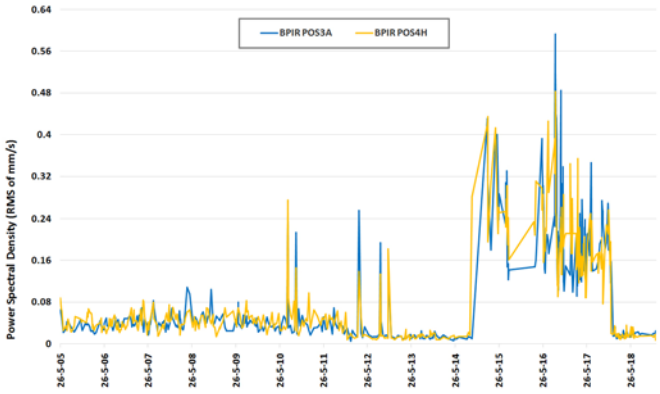

Fig. 6. BPIR result in terms of RMS (mm/s) at positions 3 axial and 4 horizontal

study of the variable 2BSF on the 3rd axis determines that the most sensitive axis in cumulative values and peaks is the vertical one, followed by the horizontal position. In the case of position 4, the most important axis is the horizontal one, followed at great distance by the vertical one.

In position 4, the highest value is obtained on the horizontal axis, followed at a great distance by the vertical and axial axis. It should be noted that the effect between the horizontal and vertical axes of position 3 and 4 is very close in cumulative terms. The analysis of the peak values determines that axis 3 vertical and 4 horizontal are the most important. These values do not exceed 1.6 RMS, being well below the critical value of 7.1 RMS.

When comparing both positions, It has been obtained that the vertical position 3 is the one that most perceives the vibration effect of this variable, followed very closely by horizontal position 4, with little more than 2 RMS difference. In terms of peak values, It has been obtained the same result (see Table 7).

Table 7. 2BSF result in terms of RMS (mm/s)

Variable	POS3H	POS3V	POS3A	POS4H	POS4V	POS4A
Total sum	88.870	119.700	40.988	117.039	69.864	49.764
Average	0.140	0.200	0.067	0.191	0.114	0.092
Peak value	1.230	1.570	0.495	1.316	1.001	0.940

The variable generated by the second harmonic of the balls follows a common pattern in positions POS3V and POS4H, even though they have different axes. This result is important and gives confidence to determine that it is possible to monitor the machine, observing the vertical position 3, as shown in Figure 7.

After evaluating the bearing frequencies, it is observed that the most determining variable is that produced by the second ball harmonic, followed by that of the cages.

The analysis of the peak values gives a more important result, obtaining in FTF 7.74 RMS a critical value of operation, making this frequency the most determinant, as shown in table number 8.

After identifying that the FTF is the most determining frequency of the SKFNU322 bearing, it is then compared with the results of the other two machine operating variables, such as SPEED and Blades.

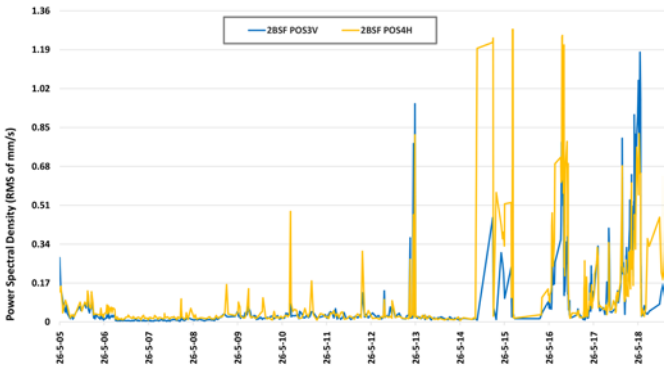

Fig. 7. Result of 2BSF in terms of RMS (mm/s) in positions 3 vertical and 4 horizontal

Table 8. Result of all bearing frequencies in terms of RMS (mm/s)

Variable	FTF POS4V	BSF POS4V	BPOR POS3A	BPIR POS3A	2BSF POS3V
Total sum	97.480	56.812	28.448	52.048	119.700
Average	0.159	0.093	0.053	0.085	0.200
Peak value	7.747	0.727	0.411	0.593	1.570

Table 9. Summary of SPEED, BLADES and FTF frequencies in terms of RMS (mm/s)

Variable	SPEED POS4V	FTF POS4V	BLADES POS3A
Total sum	1606.085	97.480	245.778
Average	2.612	0.159	0.399
Peak value	11.644	7.747	3.354

Other studies determine that the turning variable of the machine generates more incidence in POS4V. In the case of the blades, the axial position would be the most important [2, 3]. In the Table 9 shows the comparison of the three frequencies.

The graph above shows the result of SPEED, Blades and FTF, with no linearity. It is certain that this machine can be monitored through positions POS4V and POS3A, as shown in Figure 8.

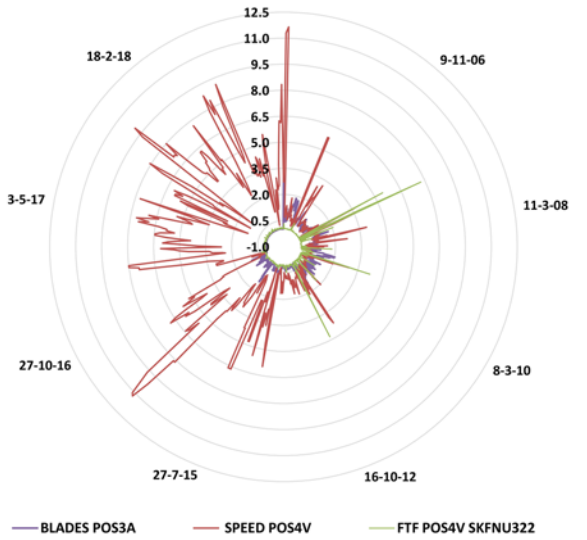

Fig. 8. Result of SPEED, FTF and Blades frequencies in terms of RMS (mm/s)

4. Conclusions

After the analysis of the variables FTF, BSF, BPOR, BPIR and 2BSF of the bearing SKFNU322, using the approximation method by power density values in accumulated values and peaks, it can be said that most important values are found in position 4, and specifically in the vertical axis.

In cumulative values, the actions created by 2BSF are the most important. However, in peak values, the most remarkable action is the one caused by FTF, with values higher than the critical ones, according to the application standard.

When comparing the FTF variable with the most representative of the machine, SPEED and Blades, it can be seen that the turning variable of the machine generates more effect in the vertical position, and the one on the blades has more effect in the axial position.

Finally, It can be concluded that despite studying 42 variables in six control points, it is possible to predict the failure of the bearing and avoid the stoppage of this equipment just monitoring POS4V and the SPEED variable.

References

1. Artzer A, Moats M, Bender J. Removal of Antimony and Bismuth from Copper Electrorefining Electrolyte: Part I, Review. Journal of The Minerals, Metals & Materials Society 2018; 70 (10): 2033-2040, https://doi.org/10.1007/s11837-018-3075-x.
2. Castilla-Gutiérrez J, Fortes JC, Pulido-Calvo I. Analysis, evaluation and monitoring of the characteristic frequencies of pneumatic drive unit and its bearing through their corresponding frequency spectra and spectral density. Eksploatacja i Niezawodnosc – Maintenance and Reliability 2019; 21 (4): 585–591, http://doi.org/10.17531/ein.2019.4.7.
3. Castilla-Gutiérrez J, Fortes JC, Davila JM. Control and prediction protocol for bearing failure through spectral power density. Eksploatacja I Niezawodnosc – Maintenance and Reliability 2020; 22 (4): 651–657, http://doi.org/10.17531/ein.2020.4.8.
4. Chaudhry V, Kailas AV. Elastic-Plastic Contact Conditions for Frictionally Constrained Bodies Under Cyclic Tangential Loading. Journal of Tribology 2013; 136 (1): 1-17, https://doi.org/10.1115/1.4025600.
5. Cong F, Chen J, Dong G. Vibration model of rolling element bearings in a rotor-bearing system for fault diagnosis. Journal of Sound and Vibration 2013; 332 (8): 2081–2097, https://doi.org/10.1016/j.jsv.2012.11.029.
6. Ding X, He Q, Luo N. A fusion feature and its improvement based on locality preserving projections for rolling element bearing fault classification. Journal of Sound and Vibration 2015; 335 (20): 367–383, https://doi.org/10.1016/j.jsv.2014.09.026.
7. Gao D, Yao W, Wu T. Failure analysis on the axial-connected bolts of the thin-walled cylinder under random vibration loading. Engineering Failure Analysis 2019; 105: 756-765, https://doi.org/10.1016/j.engfailanal.2019.06.043.
8. Gebraeel N, Elwany A, Pan J. Residual Life prediction sin the absence of prior degradation know ledge. IEEE Transaction and Reliability 2009; 58 (1): 106–117, https://doi.org/10.1109/TR.2008.2011659.
9. Goyal D, Choudhary A, Pabla BS, Dhami SS. Support vector machines based non-contact fault diagnosis system for bearings. Journal of Intelligent Manufacturing 2020; 31: 1275-1289, https://doi.org/10.1007/s10845-019-01511-x.
10. Haque T, Korres S, Carey JT, Jacobs PW, Loos J, Franke J. Lubricant Effects on White Etching Cracking Failures in Thrust Bearing Rig Tests. Engineering Optimization 2018; 61 (6): 979-990, https://doi.org/10.1080/10402004.2018.1453571.

11. Harsha SP, Nataraj C, Kankar KP. The Effect of Ball Waviness on Nonlinear Vibration Associated with Rolling Element Bearings. International Journal of Acoustics and Vibration 2006; 11 (2): 56-66, https://doi.org/10.20855/ijav.2006.11.2191.
12. Hernot X, Sartor M, Guillot J. Calculation of the stiffness matrix of angular contact ball bearings by using the analytical approach. Journal of Mechanical Design 2000; 122 (1): 83-90, https://doi.org/10.1115/1.533548.
13. Houpert L. An Enhanced Study of the Load–Displacement Relationships for Rolling Element Bearings. Journal of Tribology 2014; 136 (1): 1-11, https://doi.org/10.1115/1.4025602.
14. Houpert L. A Uniform Analytical Approach for Ball and Roller Bearings Calculations. Journal of Tribology 1997; 119 (4): 851-858, https://doi.org/10.1115/1.2833896.
15. Hsu JY, Wang YF, Lin KC, Chen MY, Hsu JHY. Wind Turbine Fault Diagnosis and Predictive Maintenance Through Statistical Process Control and Machine Learning 2020; IEEE Access, 8: 23427-23439.
16. Huang L, Huang H, Liu Y. A Fault Diagnosis Approach for Rolling Bearing Based on Wavelet Packet Decomposition and GMM-HMM. International Journal of Acoustics and Vibration 2019; 24 (2): 199-209, https://doi.org/10.20855/ijav.2019.24.21120.
17. Irwansyah D, Harahap MRF, Erliana CI, Abdullah D, Sari A, Siregar NA, Dangs A, Indahingwati A, Sumartono E, Wilujeng S, Nurmawati, Subekti P, Kurniasih N, Rosalina F and Hartono H. Improvement Suggestion Performance of Blowing Machine Line 4 with Total Productive Maintenance (TPM) Method at PT. Coca-Cola Amatil Indonesia Medan Unit. Journal of Physics: Conference Series 2019; 1361, https://doi.org/10.1088/1742-6596/1361/1/012053.
18. Kauschinger B, Schroeder S. Uncertainties in Heat Loss Models of Rolling Bearings of Machine Tools. Procedia CIRP 2013; 46: 107-110, https://doi.org/10.1016/j.procir.2016.03.168.
19. Li H, Fu L, Zheng H. Bearing fault diagnosis based on amplitude and phase map of Hermitian wavelet transform. Journal of Mechanical Science and Technology 2011; 25 (11): 2731–2740, https://doi.org/10.1007/s12206-011-0717-0.
20. Louhichi R, Sallak M, Pelletan J. A Maintenance Cost Optimization Approach: Application on a Mechanical Bearing System. International Journal of Mechanical Engineering and Robotics Research 2020; 9 (5): 658-664, https://doi.org/10.18178/ijmerr.9.5.658-664.
21. Madoliat R, Ghanati MF. Theoretical and Experimental Study of Spindle Ball Bearing Nonlinear Stiffness. Journal of Mechanics 2013; 29 (4): 633-642, https://doi.org/10.1017/jmech.2013.48.
22. Malla C, Panigrahi I. Review of Condition Monitoring of Rolling Element Bearing Using Vibration Analysis and Other Techniques. Journal of Vibration Engineering & Technologies 2019; 7: 407–414, https://doi.org/10.1007/s42417-019-00119-y.
23. McFadden PD, Smith JD. Model for the vibration produced by a single point defect in a rolling element bearing. Journal of Sound and Vibration 1984; 96 (1): 69–82, https://doi.org/10.1016/0022-460X(84)90595-9.
24. Medrano ZY, Perez C, Gomez J, Vera M. Novel Methodology of Fault Diagnosis on Bearings in a Synchronous Machine by Processing Vibroacoustic Signals Using Power Spectral Density. Ingeniería Investigación y Tecnología 2016; 17 (1): 73-85, https://doi.org/10.1016/j.riit.2016.01.007.
25. Mercorelli P. A denoising procedure using wavelet packets for instantaneous detection of pantograph oscillations. Mechanical Systems and Signal Processing 2013; 35 (1-2): 137–149, https://doi.org/10.1016/j.ymssp.2012.09.001.
26. Mucka P, Juraj Stein G, Tobolka P. Whole-body vibration and vertical road profile displacement power spectral density. Engineering Optimization 2019; 58 (4): 630-656, https://doi.org/10.1080/00423114.2019.1595675.
27. Nagi G, Alaa E, Jing P. Residual Life prediction sin the absence of prior degradation know ledge, IEEE Transaction and Reliability 2009; 58: 106–117, https://doi.org/10.1109/TR.2008.2011659.
28. Nandi S, Toliyat HA, Li X. Condition Monitoring and Fault Diagnosis of Electrical Motors-A Review. IEEE Transactions on Energy Conversion 2005; 20 (4): 719-729, https://doi.org/10.1109/TEC.2005.847955.
29. Pawlik P. Single-number statistical parameters in the assessment of the techinical condition of machines operating under variable load. Eksploatacja i Niezawodnosc - Maintenance and Reliability 2019; 21 (1): 164-169, http://doi.org/10.17531/ein.2019.1.19.
30. Qiu H, Lee J, Lin J, Yu G. Wavelet filter-based weak signature detection method and its application on rolling element bearing prognostics. Journal of Sound and Vibration 2006; 289 (4-5): 1066–1090, https://doi.org/10.1016/j.jsv.2005.03.007.
31. Schnabel S, Marklund P, Larsson R, Golling S. The Detection of Plastic Deformation in Rolling Element Bearings by Acoustic Emission. Tribology International 2017; 110: 209-215, https://doi.org/10.1016/j.triboint.2017.02.021.
32. Sawalhi N, Randall RB. Helicopter gearbox bearing blind fault identification using a range of analysis techniques. Engineering Optimization 2015; 5 (2): 157-168, https://doi.org/10.1080/14484846.2008.11464544.
33. Shahgoli G, Saunders C, Fielke J. Application of Power Spectral Density to Recognise the Important Factors Creating Tractor-Subsoiler Vibrations. Engineering Optimization 2015; 7 (1): 39-46, https://doi.org/10.1080/14488388.2009.11464797
34. Sun Q, Feng D, He L, Tu Y, Zhang H, Shi L. Failure analysis of cantilever bearing in wellbore trajectory control tool with high build-up rate. Engineering Failure Analysis 2019; 104: 1040-1052, https://doi.org/10.1016/j.engfailanal.2019.06.024.
35. Toledo E, Pinhas I, Aravot D, Akselrod S. Bispectrum and bicoherence for the investigation of very high frequency peaks in heart rate variability. Proceedings of the IEEE Computers in Cardiology 2001; 28: 667-670, https://doi.org/10.1109/CIC.2001.977744.
36. Tse P, Peng Y, Yam R. Wavelet analysis and envelope detection for rolling element bearing fault diagnosis-Their Effectiveness and Flexibilities. Journal of Vibration and Acoustic 2001; 123 (3): 303-310, https://doi.org/10.1115/1.1379745.
37. Vitturi S. PC-based automation systems: an example of application for the real-time control of blowing machines. Computer Standars and Interfaces 2004, 24: 145-155, https://doi.org/10.1016/S0920-5489(03)00063-1.
38. Wang J, Liang Y, Zheng Y, Gao RX, Zhang F. An integrated fault diagnosis and prognosis approach for predictive maintenance of wind turbine bearing with limited samples. Renewable Energy 2020; 145: 642-650, https://doi.org/10.1016/j.renene.2019.06.103.
39. Wang NF, Jiang DX, Yang WG. Dual-Tree Complex Wavelet Transform and SVD-Based Acceleration Signals Denoising and its Application in Fault Features Enhancement for Wind Turbine. Journal of Vibration Engineering & Technologies 2019; 7: 311–320, https://doi.org/10.1007/s42417-019-00126-z.
40 . Yeong-Maw H, Dyi-Cheng C, Gow-Yi T. Study on Asymmetrical Sheet Rolling by the Finite Element Method. Journal of Mechanics 1999; 15 (4): 149-155, https://doi.org/10.1017/S1727719100000435.
41. Yujie G, Jingyu L, Jie L, Zhanhui L, Wentao Z. A method for improving envelop spectrum symptom of fault rolling bearing based on the auto-correlation acceleration signal. Applied Mechanics and Materials 2013; 275-277: 856–864, https://doi.org/10.4028/www.scientific.net/AMM.275-277.856.

42. Zheng D, Chen W. Thermal performances on angular contact ball bearing of high speed spindle considering structural constraints under oil-air lubrication. Tribology International 2017; 109: 593–601, https://doi.org/10.1016/j.triboint.2017.01.035.
43. Zhou W, Habetler TG, Harley RG. Bearing Condition Monitoring Methods for Electric Machines: A General Review. IEEE International Symposium on Diagnostics for Electric Machines, Power Electronics and Drives 2007; 3-6, https://doi.org/10.1109/demped.2007.4393062.